# Development and Evaluation of a Monte Carlo Technique for the Simulation of Multifunctional Polymerizations

**Devdatt L. Kurdikar,[†,‡,§] Jan Šomvársky,[‡] Karel Dušek,[‡] and Nikolaos A. Peppas*[,†]**

*School of Chemical Engineering, Purdue University, West Lafayette, Indiana 47907-1283, and Institute of Macromolecular Chemistry, Czech Academy of Sciences, 16206 Prague 6, Czech Republic*

*Received December 15, 1994; Revised Manuscript Received May 1, 1995[⊗]*

ABSTRACT: A stochastic simulation technique was developed to describe the kinetic behavior of bulk multifunctional photopolymerizations and the structural evolution of the polymer networks. Rate equations were written for each of the reacting species. In cross-linking polymerizations, the initiator efficiency, $f$, and the propagation and termination rate constants, $k_p$ and $k_t$, are diffusion-dependent from the onset of the reaction. We were able to calculate $f$, $k_p$, and $k_t$ throughout the simulation using previously developed models. From a waiting time distribution, the time between two consecutive reactions was computed. A specific reaction pathway was chosen from knowledge of the reaction probability density function. Corresponding changes were made in the molecular distribution. With such an approach, we were able to obtain kinetic as well as structural information. The results presented here simulate the bulk polymerization of diethylene glycol diacrylate containing 1% 2,2-dimethoxy-2-phenylacetophenone as the photoinitiator. The simulation was able to predict experimentally observed reaction trends.

## Introduction

When multifunctional monomers are polymerized in bulk, they form rigid, glassy polymer networks. These polymers are used in the coatings, films, and packaging industries, as materials for information storage systems, and aspherical lenses,[1] and as biomaterials.[2,3] These materials are usually prepared by free-radical polymerizations and typically initiated with UV light since photoinitiation offers good spatial and temporal control.

The free-radical mechanism is fairly well understood; however, predictive models that can describe both the kinetic and structural characteristics of the network are lacking. This is because bulk cross-linking polymerizations possess some features which are less prominent or are absent in linear polymerizations. These include (i) the presence of microgel-like particles or spatial heterogeneities,[4] (ii) diffusion-dependent propagation and termination rate constants, and (iii) different conversion-dependent reactivities of pendant double bonds and the double bonds in free monomer molecules.[5,6]

Several kinetic models have been proposed to explain some of these characteristics, most of which are directly or indirectly caused by diffusional limitations on the reacting species. One of the widely used models was developed by Marten and Hamielec[7] who used the Doolittle expression for the diffusivity of a small molecule in a polymer solution to derive equations that could be used to calculate the rate constants throughout the whole range of conversion. Though these equations[7] were originally derived for the modeling of linear polymerizations, they have also been used in the modeling of cross-linking reactions.[8,9]

Soh and Sundberg[10−13] used an approach similar to that of Marten and Hamielec but also accounted for the mobility of the radicals due to propagation reactions. Batch and Macosko[14] recently presented a model for cross-linking reactions and included the diffusional effects on the reaction process. They included the changing initiator efficiency and accounted for the different co-existing radical populations using semiempirical equations. Disadvantages of these approaches include the need for evaluation of empirical parameters involved in the models and the inability to make quantitative predictions regarding the structural characteristics of the final networks.

Predictions for the structural features of the networks have been obtained using statistical methods[15,16] or the pseudokinetic rate constant method.[17,18] Tobita and Hamielec[19] also presented a model that was based on the cross-linking density distribution of primary polymer molecules that results during network formation; they successfully applied the model to the batch copolymerization of methyl methacrylate/ethylene glycol dimethacrylate. Using the cross-linking density distribution as a basis, Tobita[20,21] simulated the network formation process for the case of kinetically controlled cross-linking copolymerization and was able to obtain structural information such as the weight fraction of the sol and the gel and the molecular weight distribution. However, the use of these theories requires a knowledge of the reaction rate constants over the whole range of conversion and the kinetic information obtained from such models is often sparse.

In addition to diffusion control, cyclization is another important issue in network formation by free-radical cross-linking copolymerizations particularly at the beginning of the reaction. Its intensity is determined by the chance that a free radical at the end of the growing chain meets a pendant double bond in the same molecule relative to the chance of meeting a double bond bonded to another molecule. Due to the specific reaction mechanism—a fast propagation rate—the chance for cyclization diverges in the limit of zero polymerization conversion just because there are no *other* macromolecules available when the first one is growing relative

* Corresponding author.
† Purdue University.
‡ Czech Academy of Sciences.
§ Present address: Monsanto Co. Corporate Research, Mail Zone Q3F, 800 N. Lindbergh Blvd., St. Louis, MO 63167.
⊗ Abstract published in *Advance ACS Abstracts,* July 15, 1995.

0024-9297/95/2228-5910$09.00/0 

to the chance of meeting a pendant double bond attached to another macromolecule. Cyclization is thus the most important special feature of the structure growth. In order for a bond to be formed, the two reacting sites must be present within a reaction volume. For cyclization, the probability that this happens depends on the length and flexibility of the connecting path(s) (static effect) and on the sites interdiffusion rate (dynamic effect).

Because of the importance of cyclization, the problem deserves a deeper comment. The evolution of molecular species in the classical ("ring-free") mean field kinetic description is determined by the mass action law. The rate of transformation of a given species by reactions with other species is assumed to be proportional to the products of *average concentrations* (in the whole volume) of groups of this species and concentration of groups of all existing molecules. These products involve also squares of average group concentrations of the same molecule within the whole volume (disregarding the correlation of group distances due to molecule connectivity) which describe the rate of formation of bonds within the same molecules—cyclization. However, in the limit of an infinite system the intensity of these cyclization reactions is zero in all finite molecules with the exception of the largest (infinite) one—the gel. Assuming the validity of the mass action law applied to average concentrations, these intramolecular reactions in the gel are responsible for the buildup of cycle rank or cross-linked concentration in the gel "molecule".[22] If these intramolecular reactions are prohibited, the treelike structure growth continues beyond the gel point until a certain limiting conversion is reached and all material is contained in the infinite treelike molecule.[23] In a finite system, however, the intramolecular reactions within individual molecules are not negligible.[24,25] With increasing system size their intensity converges to zero except for the largest molecule beyond the gel point.

This type of cyclization called *uncorrelated circuit closing*[26] occurs only in the gel and represents the base for classical calculation of postgel properties (sol fraction, concentration of elastically active network chains, etc.).[22] This approach tacitly assumes that connections between near and distant groups within the gel molecule are equally probable. In many real systems and in free-radical polymerizations in particular, cyclization can be strong even in finite molecules. A physically sound approach should consider both the static and kinetic factors: the probability that the two sites occur within the same reaction volume when the diffusion is fast (static or conformational factor) and the diffusion-controlled mutual approach of the two sites from their equilibrium positions (dynamic effect). The static effect dominates low-conversion reactions; diffusion control becomes dominant near and beyond the gel point. The overall cyclization rate constant, $k_c$, will have the form

$$\frac{1}{k_c} = \sum \frac{1}{k_{c,stat,i}} + \sum \frac{1}{k_{c,D,i}} \qquad (1)$$

where the summation extends over sites having topological distances $i$.

Most of the off-space simulations considered the static (conformational) factors when diffusion limitations were not significant,[27-30] sometimes just by adding an extra term headed by an empirical cyclization constant independent of conversion.[31] Other authors considered in the postgel region the uncorrelated circuit closing without diffusion control[32,33] or controlled by diffusion.[34]

Dušek and Šomvársky,[25,35] proposed to use the kinetic (coagulation) theory for cyclization complicated by excluded volume effects and diffusion. Formation of cycles is intrinsic for simulations in space and will be mentioned below.

The analysis of cyclization is not the main issue of this work; we will consider here just the uncorrelated circuit closing affected by diffusion. Since diffusion affects inter- and intramolecular reactions differently, it is not clear whether cyclization relative to the intermolecular reaction is still asymptotically negligible in the limit of the infinite system or not. This will be analyzed in the future.

Space-based simulation models have also been developed to qualitatively describe the polymerization kinetics and the structural evolution of the network. Lattice-based[36,37] and off-lattice-based models[38-41] have been developed for this purpose. Boots and co-workers[6,42,43] pioneered the use of lattice-based models to predict the enhanced reactivity of pendant double bonds at low conversion during a tetrafunctional polymerization and demonstrate the formation of microgels. Subsequent advances accounted for variation in initiation rates,[44,45] the presence of a solvent,[46] and the mobility of the reacting species.[46,47] Recently, lattice-based models have been used for studying cyclization reactions in multifunctional polymerizations[48] and the formation of microgels.[49] As these models are most suited for situations where relaxation to the equilibrium state is slow with respect to growth, effects such as termination due to segmental diffusion and volume shrinkage due to polymerization are not included.[44] Hence, they have restricted applicability for the prediction of kinetic behavior of cross-linking reactions. Space-based simulation involving diffusion control was offered also by Chiu and Lee,[50] but its predictive value is limited by the two-dimensionality of the space in which the simulation was carried out.

Off-space Monte Carlo simulations of polymerization reactions offer the possibility of simultaneously obtaining kinetic and structural information. These simulations are based on the algorithm presented by Gillespie[51,52] who used a Monte Carlo approach to numerically calculate the time evolution of a mixture of molecular species that interact through a set of specified reaction channels. This method allows the normally intractable "master equation", which results from a stochastic treatment of chemical reactions,[53] to be numerically treated even for complex reacting systems. Additionally, assumptions such as the quasi-steady-state approximation for the radical concentration that are usually made in the modeling of polymerization reactions are not necessary. Recently, such an approach has been used for studying pulsed-laser initiated polymerizations[54] and the curing of epoxides with amines.[55] These researchers however did not include a predictive model for the determination of rate constants throughout the polymerization process in their simulations.

In this paper, we present the derivation of a kinetic model and an off-space stochastic computer simulation of a bulk tetrafunctional polymerization using the new kinetic model. This model incorporates conversion-dependent initiator efficiency and rate constants. Since the time evolution of each of the molecular species present in the reaction mixture is followed in this simulation technique, kinetic as well as structural

information is obtained simultaneously. This information is compared with experimentally observed reaction trends. The effects of variations in the photoinitiation rate on the reaction characteristics are also analyzed. To the best of our knowledge, this is the first effort to use a physical model-based Monte Carlo simulation algorithm to understand and describe the bulk multifunctional photopolymerization process.

## Model Description

Free-radical polymerizations follow the initiation, propagation, and termination scheme typical of chain reactions. In the initiation step, the initiator splits up into two equal or unequal radicals which react with the unsaturated C=C double bonds to form active or "live" monomers. In the propagation step, unreacted monomer units attach to a "live" monomer to form a growing chain. In the termination step, two active monomers react by a bimolecular mechanism to form inactive polymer chain(s).

The above reaction mechanism is valid for a system in which chain transfer reactions are either absent or suppressed. It was assumed that termination was by combination only; such an assumption is valid for most polymerizations. However, some traditional assumptions made in the modeling of polymerizations such as a diffusion-independent and constant value for initiator efficiency throughout the reaction and the quasi-steady-state approximation for the radical concentration were not made in the model developed here.

**Initiation.** For photoinitiated polymerizations occurring in a thin film, the rate of initiator decomposition, $R_A$, can be calculated[9] as

$$R_A = I_0 \epsilon [A] \tag{2}$$

Here, [A] is the initiator concentration at time $t$, $I_0$ is the incident light intensity, and $\epsilon$ is the extinction coefficient. Since the dissociation of an initiator typically leads to the formation of two radicals, the rate of primary radical formation is twice that of the initiator decomposition rate.

As explained below, only a fraction of all radicals produced leads to the formation of propagating chains; this fraction is given by the quantum yield for initiation, $\phi$. The term $\phi$ is defined as the number of propagating chains produced per light photon absorbed and can be expressed as $\phi = f\phi'$, where $f$ is the initiator efficiency and $\phi'$ is the number of initiator molecules dissociated per light photon absorbed. The initiator efficiency is defined as the fraction of radicals produced upon initiator decomposition that actually initiates propagating chains.

The initiator used in our previous experimental investigation[56] was 2,2-dimethoxy-2-phenylacetophenone (DMPA). On decomposition, this initiator splits into two unequal radicals: the benzoyl and the benzoyl ketal radical.[57,58] The benzoyl ketal radicals may either recombine with the benzoyl radicals or decompose further to form methyl radicals and methyl benzoate. The methyl radicals and the benzoyl radicals are instrumental in initiating chains. However, recombination reactions between the primary radicals often lead to the formation of inactive initiator molecules which on decomposition do not lead to the formation of active radicals.

Due to these recombination reactions, not all the primary radicals are successful in initiating chains. Additionally, some primary radicals terminate growing chains rather than initiating new ones. These reactions lead to a decrease in the initiator efficiency. Recombination reactions become more frequent as the polymerization proceeds because of the decrease in the radical diffusivity associated with an increase in the volume fraction of polymer in the reacting mass. Thus, the initiator efficiency decreases as the reaction progresses until it approaches a value of zero at limiting conversions as has been experimentally shown by other investigators.[59,60]

A model has been previously developed by us[61] to relate the initiator efficiency, $f$, to the radical diffusivity. The following assumptions were made to simplify the model without a significant loss in its predictive capabilities: (i) all radicals had the same diffusivity; (ii) the radius of the solvent cage around each radical was the same; and (iii) the recombination reaction rate constants were approximately equal. The resulting equation is as follows:

$$f = \left[1 - \frac{ak_{i,1}}{D_A + ak_{i,1} + a\sqrt{k_{d,r,1}D_A}}\right] \times \left[1 - \frac{a^2 k_{i,1} k_{d,r,1}}{[\sqrt{\hat{k}/D_A} + \sqrt{k_{d,r,1}/D_A}]} \frac{1}{[D_A + ak_{i,1} + a\sqrt{k_{d,r,1}D_A}]} \times \frac{1}{[D_A + ak_{i,1} + a\sqrt{\hat{k}D_A}]}\right] \tag{3}$$

Here, $a$ is the radius of the solvent cage (i.e. the volume around one radical within which another radical may recombine), $D_A$ is the relative diffusivity of the primary radicals, $k_{i,1}$ is the radical recombination reaction specific rate constant, and $k_{d,r,1}$ is the rate constant for the decomposition of the benzoyl ketal radical into methyl benzoate and the methyl radical. The term $\hat{k}$ was written as

$$\hat{k} = k_{p,1}[M] + k_{t,1}[M^\bullet] \tag{4}$$

where $k_{p,1}$ is the rate constant for the reaction of a primary radical with an unreacted monomer and $k_{t,1}$ is the rate constant for the reaction of a primary radical with a growing polymer chain. Typically, $k_{p,1}[M] \gg k_{t,1}[M^\bullet]$, and therefore only the first term was used in the calculation of $\hat{k}$.

The relative diffusivity was calculated as $D_A = 2D_r$ where $D_r$ is the diffusivity of the radical in the polymerizing mixture. The term $D_r$ was estimated during the reaction simulation by using the Vrentas–Vrentas theory[62] for the diffusion of penetrants in cross-linked polymers.

**Propagation.** The propagation step involves the reaction of a radical with a double bond by either an intramolecular or an intermolecular route. An intramolecular reaction is one in which a radical and a pendant double bond, both of which are a part of the same macromolecule react. In an intermolecular reaction, the radical and the double bond are attached to different polymer molecules. However, in each case the intrinsic reaction mechanism is bimolecular.

The rate of propagation was written as

$$R_p = k_p[M][M^\bullet] \tag{5}$$

where $R_p$ is the rate of propagation, $k_p$ is the propaga-

tion rate constant, [M] is the monomer concentration, and [M•] is the radical concentration. If the long chain hypothesis which states that the loss of monomer units is primarily due to propagation reactions is invoked, eq 5 can also be used to calculate the polymerization rate.

Propagation reactions are thought to occur in three consecutive steps. First, the monomer or the macromolecule containing the double bond undergoes translational diffusion toward the radical site. Then, segmental diffusion causes the (meth)acryl group to be oriented toward the radical site, followed by the chemical reaction between the two reacting moieties. For intramolecular termination reactions, only the segmental diffusion and chemical reaction steps are involved.

The diffusion-controlled propagation rate constant was written as a sum of the reaction resistances as

$$\frac{1}{k_p} = \frac{1}{k_{p,trans}} + \frac{1}{k_{p,seg}} \tag{6}$$

where $k_{p,trans}$ and $k_{p,seg}$ are the translational and segmental diffusion contributions to the propagation rate constant, respectively. A more general equation (7) includes the chemically controlled propagation reaction

$$\frac{1}{k_p} = \frac{1}{k_{p,trans}} + \frac{1}{k_{p,seg}} + \frac{1}{k_{p,ch}} \tag{7}$$

governed by the rate constant in the region where $k_{p,trans}, k_{p,seg} \gg k_{p,ch}$. The term $k_{p,ch}$ exhibits the Arrhenius dependence on temperature and is governing linear polymerizations and sometimes the early stages of polyvinyl polymerizations before the glass transition is reached. Knowing that diffusional limitations set in much earlier in cross-linking polymerizations than they do in linear polymerizations, a diffusion-controlled mechanism was assumed from the onset of the reaction. As experimental data on $k_{p,ch}$ become available, the presence of chemical control at the very early stages of the reaction can be incorporated into the simulation.

Each of the diffusional contributions was written in terms of the Smoluchowski rate expression which relates[63] the reaction rate constant to the diffusivities of the reacting species as

$$k_{p,trans} = 4\pi R(D_{i,t} + D_{j,t}) \tag{8}$$

where $R$ is the effective reaction radius and $D_{i,t}$ and $D_{j,t}$ are the translational diffusivities of the two reacting species having degrees of polymerization $i$ and $j$, respectively. A similar expression for the segmental contribution is

$$k_{p,seg} = 4\pi R(D_{i,s} + D_{j,s}) \tag{9}$$

where $D_{i,s}$ and $D_{j,s}$ are the segmental diffusivities of the two reacting species having degrees of polymerization $i$ and $j$, respectively.

The monomer diffusivity was calculated using the Vrentas and Vrentas[62] extension of the Vrentas and Duda theory[64,65] for the diffusion of penetrants in polymer–solvent systems. This theory has been applied to lightly cross-linked polymers having at least 50 bond vectors between cross-links. When more appropriate predictive theories for diffusion in highly cross-linked materials become available, they can be used instead of the Vrentas–Duda theory. However, at this point, the Vrentas–Duda theory is sufficient. The solvent self-diffusion coefficient, $D_1$ was related to the polymer and solvent mass fractions, $\omega_i$, as follows:

$$D_1 = D_0 \exp\left[-\frac{E}{RT}\right] \exp\left[-\frac{\gamma(\omega_1 \hat{V}_1^* + \omega_2 \xi \hat{V}_2^*)}{\hat{V}_{FH}}\right] \tag{10}$$

Here, $D_0$ is a constant pre-exponential factor, $E$ is the energy per mole that a molecule needs to overcome attractive forces that hold it to its neighbor, $T$ is temperature, $\gamma$ is an overlap factor introduced to account for the fact that the same free volume is available to more than one molecule ($0.5 < \gamma < 1.0$), $\hat{V}_i^*$ is the specific critical hole volume of component $i$ required for a jump, $\xi$ is the ratio of the critical molar volume of the solvent jumping unit to the critical molar volume of the polymer jumping unit, and $\hat{V}_{FH}$ is the average hole free volume per gram of mixture, where the subscripts 1 and 2 designate the monomer and polymer, respectively.

The term $\xi$ can be calculated as

$$\xi = \frac{\hat{V}_1^* M_{j1}}{\hat{V}_2^* M_{j2}} \tag{11}$$

where $M_{ji}$ is the molecular weight of a jumping unit of component $i$.

For cross-linked systems, the following equation was used for the equilibrium calculation of $\hat{V}_{FH}$.

$$\hat{V}_{FH} = \omega_m v_m v_{fm} + \omega_p v_p(T,0) v_{fp} \delta \tag{12}$$

Here, $\omega_m$ and $\omega_p$ are the weight fractions of the monomer and polymer, $v_m$ is the specific volume of the monomer, $v_p(T,0)$ is the specific volume of the corresponding un-cross-linked polymer, $v_{fm}$ and $v_{fp}$ are the fractional free volumes of the monomer and polymer, and $\delta$ is the factor introduced by Vrentas and Vrentas[62] to account for the presence of cross-links. The term $\delta$ was calculated as

$$\delta = \frac{v_p(T,X)}{v_p(T,0)} \tag{13}$$

where $v_p(T,X)$ is the specific volume of the polymer at degree of cross-linking $X$ and temperature $T$.

Kloosterboer[1] has shown that in the course of a bulk cross-linking polymerization, a temporary excess free volume exists in the reacting system as a result of a lag between the volumetric shrinkage rate and the reaction rate. In a mean field treatment, this excess free volume can be estimated using the method of Bowman and Peppas[9] and added to the equilibrium free volume; thus the actual free volume can be calculated. However, we are unaware of a practical non mean field method to calculate the excess free volume and hence the equilibrium free volume was used in this investigation.

Since models to predict the translational diffusivity of branched and/or cross-linked macromolecules in a polymerizing system are not available, the following equation was used to calculate it.

$$D_{i,t} = \frac{D_{1,t}}{i^n} \tag{14}$$

Here, $D_{i,t}$ is the diffusivity of the branched/cross-linked macromolecule in the reacting system, $D_{1,t}$ is the diffusivity of the monomer in the polymer–solvent system as calculated by the Vrentas–Vrentas theory, and $i$ is the degree of polymerization of the diffusing macromol-

ecule. According to de Gennes,[66] the diffusivity of a linear chain in an entangled system is proportional to $i^{-2}$; hence, $n = 2$ was used in the present work. When experiments elucidate the exact value of $n$, it can be used in future simulation efforts.

The segmental diffusion coefficient, $D_{seg}$, was calculated as

$$D_{seg} = pD_{1,t} \tag{15}$$

where $p$ is the probability that one of the double bonds of the monomer is oriented toward a radical site. The probability was estimated to be on the order of $10^{-4}$, as shown earlier.[67] It is known that in the initial stages of linear polymerizations, the segmental diffusivity of active chains may not change appreciably with conversion,[68] and hence the value of $D_{seg}$ was maintained at a constant value calculated at the onset of the reaction. Also, for lack of a predictive model to calculate the segmental diffusivity of a branched macromolecule during the course of the reaction, it was assumed that $D_{i,s} = D_{seg}$. As better theoretical models for the prediction of the diffusivity of segments of a branched/cross-linked macromolecule become available, they can be included in the simulation technique reported here.

With these expressions we were now able to calculate the rate of propagation using eq 5, for each reactive pair of molecules.

**Termination.** The termination step also may be either intramolecular or intermolecular, as described earlier, except that in this case the reaction occurs between two radicals. The rate of termination was calculated as follows

$$R_t = k_t[M^\bullet]^2 \tag{16}$$

where $R_t$ is the rate of termination and $k_t$ is the termination rate constant. The termination rate constant was calculated according to the procedure outlined earlier for the calculation of $k_p$ (eqs 6–15).

In multifunctional polymerizations, "propagation diffusion" may be an important mode of mobility for the radicals. In this mode, radical movement is increased due to the displacement of the radical because of propagation reactions. This effect was difficult to include in the simulation and has been neglected at present.

This completes the derivation of the model. The diffusivity dependence of the initiator efficiency and the propagation and termination rate constants were incorporated. Rate equations (2), (5), and (16) were used to calculate the initiation, propagation, and termination rates, for each pair of reactive species, respectively.

## Simulation Technique

Though the technique outlined here can be used for a variety of linear and cross-linking polymerizations, it was used here for the simulation of a free-radical homopolymerization of a tetrafunctional monomer such as a di(meth)acrylate.

**Fundamentals.** The tetrafunctional monomer is presumed to be in one of the six states shown in Figure 1. In state M, the monomer is completely unreacted; in state $A_1$, one double bond is unreacted and the other has a radical present; in state $A_2$, both double bonds have reacted and have radicals present; in state $A_3$, one double bond is completely reacted and the other is unreacted; in state $A_4$, one double bond is completely reacted and the other has a radical present; and, in state $A_5$, both double bonds are completely reacted. No distinction is made between monomer units which are in the same state but are attached to molecules of different sizes. Such a representation has been used previously by other investigators.[69,70]

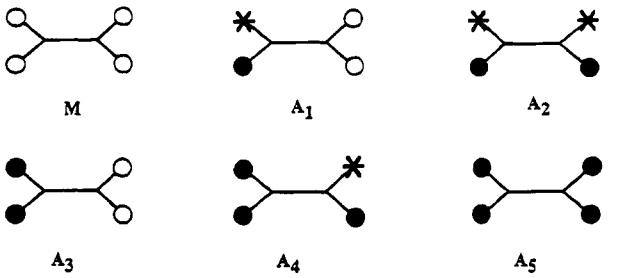


**Figure 1.** Schematic of the six states that the monomer units are presumed to be in. The ○– represents an unreacted bond, ●– represents a reacted bond, and *– represents a radical.

**Table 1. Initiator Decomposition Reaction and the Propagation (P) and Termination (T) Reactions That May Occur during a Tetrafunctional Polymerization[a]**

| reacn | P/T | intermolecular reacn no. | intramolecular reacn no. |
|---|---|---|---|
| $M + A_1 \rightarrow A_1 + A_3$ | P | 1 | |
| $M + A_2 \rightarrow A_1 + A_4$ | P | 2 | |
| $M + A_4 \rightarrow A_1 + A_5$ | P | 3 | |
| $A_1 + A_2 \rightarrow A_2 + A_4$ | P | 4 | 16 |
| $A_1 + A_2 \rightarrow A_3 + A_4$ | T | 5 | 17 |
| $A_1 + A_3 \rightarrow A_3 + A_4$ | P | 6 | 18 |
| $A_1 + A_4 \rightarrow A_2 + A_5$ | P | 7 | 19 |
| $A_1 + A_4 \rightarrow A_3 + A_5$ | T | 8 | 20 |
| $A_2 + A_3 \rightarrow A_4 + A_4$ | P | 9 | 21 |
| $A_2 + A_4 \rightarrow A_4 + A_5$ | T | 10 | 22 |
| $A_3 + A_4 \rightarrow A_4 + A_5$ | P | 11 | 23 |
| $A_1 + A_1 \rightarrow A_2 + A_3$ | P | 12 | 24 |
| $A_1 + A_1 \rightarrow A_3 + A_3$ | T | 13 | 25 |
| $A_2 + A_2 \rightarrow A_4 + A_4$ | T | 14 | 26 |
| $A_4 + A_4 \rightarrow A_5 + A_5$ | T | 15 | 27 |
| $A \rightarrow 2A_1$ | | | 28 |

[a] These reactions could be intermolecular or intramolecular.

Macromolecules were differentiated on the basis of the number of monomer units in each of the five reacted states that they contained, and not simply on the total number of monomer units in the macromolecule or the degree of polymerization. In reality, it is possible that two macromolecules may contain the same number of monomer units in each of the states $A_1$–$A_5$ but may have completely different conformations and structure. However, this fine distinction was not made in this work because of the lack of predictive theories that can differentiate to this detail in the calculation of diffusional characteristics.

Each of the various reactions that are possible in the course of a free-radical homopolymerization are shown in Table 1. These reactions may be either propagation reactions or termination reactions and may be either intermolecular or intramolecular. Each of these possibilities was separately accounted for and assigned a specific reaction number, as shown in Table 1. Reactions 1–15 are intermolecular, reactions 16–27 are intramolecular and lead to the formation of cycles, and reaction 28 is the initiator decomposition reaction. Among the intermolecular reactions, reactions 1–3 are the addition of a free unreacted monomer unit to a growing macromolecule, while the rest are reactions between two polymer molecules.

The presence of primary radicals was not directly accounted for in this simulation. Instead, it was assumed that the decomposition of an initiator molecule,

A, leads to the formation of two monomer units in state $A_1$ with a probability given by the quantum yield for initiation, $\phi$.

**Algorithm.** An initial molecular distribution for the bulk polymerization consisting of di(meth)acrylates $N_0$ (i.e. monomer units in state M) and $A_0$ initiator molecules was used at the start of the simulation. Several counters such as the reaction time and the number of reactions were initialized to zero.

Knowing the molecular distribution, the conversion and the weight fractions of the monomer and polymer were calculated. In the first iteration, the conversion was zero and the weight fraction of the monomer was unity. Then, the monomer and radical diffusivities were calculated using the Vrentas–Vrentas theory described earlier. The segmental diffusivity was also calculated using eq 15. Though no oligomers or polymers were present at the start of the reaction, they were formed during the polymerization process. When they were present, the diffusivity of each type of macromolecule present in the reacting mass was calculated according to eq 14 in each iteration of the algorithm.

Once the diffusivities of all molecules were known, the rate constant and the intrinsic reaction rate for each of the 28 reactions (see Table 1) was calculated for each pair of molecule types. Equations 2, 5, and 16 were used to calculate the rates of initiator decomposition, propagation, and termination, respectively.

Next, the specific reaction, $\mu$, between a specific pair of molecule types that will occur in a time interval $(t, t + \tau)$ was calculated according to a procedure given by Gillespie.[51,52]

$$\sum_{v=1}^{\mu-1} R_v < r_1 R_{\text{Tot}} \leq \sum_{v=1}^{\mu} R_v \tag{17}$$

Here, $R_v$ is the rate through reaction channel $v$, i.e. the rate of reaction of type $i$, between a molecule of type $j$ and a molecule of type $k$ (k = 0 if the reaction is intramolecular), $r_1$ is a uniformly distributed random number in the interval [0,1], and $R_{\text{Tot}}$ is the total reaction rate calculated as

$$R_{\text{Tot}} = \sum_{v=1}^{\alpha} R_v \tag{18}$$

Here, $\alpha$ is the total number of reactions that can occur between all molecular species, i.e., the total number of reaction channels.

If desired, the probability of the occurrence of a particular reaction, $P_\beta$, can simply be calculated as

$$P_\beta = \frac{R_\beta}{R_{\text{Tot}}} \tag{19}$$

where $\beta$ is the specific reaction channel and $R_\beta$ is its rate.

To be able to calculate the waiting time between two successive reactions, a waiting time distribution is required. This distribution was derived as follows. A brief description is given here; a rigorous theoretical analysis has been given by Gillespie.[51,52]

Let $F_T(\tau)$ be the waiting time cumulative distribution function. Then, $F_T(\tau)$ is the probability that T $\leq \tau$ and was represented as

$$F_T(\tau) = \Pr\{T \leq \tau\} \tag{20}$$

Therefore, it follows that

$$1 - F_T(\tau) = \Pr\{T > \tau\} \tag{21}$$

Therefore the probability that $T > \tau + \Delta\tau$ was given by

$$\Pr\{T > \tau + \Delta\tau\} = \Pr\{T > \tau\} \Pr\{\text{no reaction occurs between } \tau \text{ and } \tau + \Delta\tau\} \tag{22}$$

which led to

$$1 - F_T(\tau+\Delta\tau) = [1 - F_T(\tau)][1 - \sum_{r=1}^{\alpha} c_r p_r \Delta\tau] \tag{23}$$

Here, $c_r$ is the number of distinct combinations of the reacting pair of molecules and $p_r\Delta\tau$ is the average probability that a particular pair of reactant molecules of the $r$th reaction will react in the next infinitesimal time interval, $\Delta\tau$. Also, $p_r$ is related to the reaction rate constant, $k_r$, as $p_r = k_r/V$, where $V$ is the volume of the reacting mass,[51] and for the case of a reaction between molecules of type 1 and type 2, $c_r$ is simply $N_1N_2$, where $N_i$ is the number of molecules of type $i$ in the system.

Equation 23 leads to

$$\frac{d}{d\tau}[1 - F_T(\tau)] = -[1 - F_T(\tau)]\sum_{r=1}^{\alpha} c_r p_r \tag{24}$$

Solution of this equation using the condition $F_T(0) = 0$ gave the waiting time distribution as

$$F_T(\tau) = 1 - \exp[-R_{\text{Tot}}\tau] \tag{25}$$

where $R_{\text{Tot}} = \sum_{r=1}^{\alpha} c_r p_r$.

The inversion technique[51] was used to generate the waiting time, $\tau$, since $F_T(\tau)$ was a monotonic function and was bounded in the interval [0,1]. Therefore, $\tau$ was chosen so that the following equality was satisfied.

$$r_2 = F_T(\tau) \tag{26}$$

Here, $r_2$ is a uniformly distributed random number over the unit interval. Then, $\tau$ was calculated by the following equation

$$\tau = -\frac{1}{R_{\text{Tot}}} \ln(1 - r_2) \tag{27}$$

or by

$$\tau = -\frac{1}{R_{\text{Tot}}} \ln(r_2) \tag{28}$$

since $(1 - r_2)$ and $r_2$ are stochastically equivalent. As the simulation progressed, the waiting time calculated between two successive reactions was stored in a cumulative manner to obtain the reaction time. This reaction time was used to obtain conversion–time data and other profiles.

At this point, a particular reaction of type $i$, between molecules of types $j$ and $k$, was identified as having occurred (i.e. a reaction channel was selected) and the associated waiting time and reaction time were determined.

Using the previously computed radical diffusivity, the initiator efficiency, $f$, was calculated using eq 3 and therefore the quantum yield for initiation, $\phi$, was obtained.

Depending on the reaction channel that was selected, appropriate changes were made in the molecular distribution. This was possible since each specific reaction number was associated with a specific reaction pathway, as shown in Table 1, and the number of monomer units in each of the reacted $A_1-A_5$ states was stored for each polymer molecule. The product molecule was compared with the pre-existing molecules in terms of the number of monomer units in each of the $A_1-A_5$ states. If the product molecule was found to be of a previously existing type, the number of molecules of that type was simply increased by unity. If the product molecule was found to be of a new type, the number of types of molecules in the reacting system was increased by 1. Reactions 1–27 (see Table 1) were treated in this manner.

If the initiator decomposition reaction (reaction 28) was identified as having occurred, a uniformly distributed unit interval random number, $r_3$, was generated. If the inequality $r_3 < \phi$ was satisfied, two monomer units were converted from the M state to the $A_1$ state, and the number of initiator molecules in the reacting system was decreased by unity. Thus, the new molecular distribution at the end of a single reaction was obtained.

This series of computations completed one iteration. The procedure is summarized as follows. First, the weight fractions of the monomer and polymer were calculated, followed by the calculation of the diffusivity of each of the species present in the reacting mass. Then, the intrinsic rate of each possible reaction pathway was calculated and a specific reaction pathway was chosen using a random number. Next, the time between two successive reactions was calculated from the waiting time distribution. From a knowledge of the chosen reaction pathway, appropriate changes were made in the molecular distribution. The procedure was repeated until the reaction goes to completion or until the reaction time exceeded a preset value (10 000 s in our work). A similar simulation technique was recently developed for kinetically controlled processes described by generalized Smoluchowski coagulation equations[25] and used to simulate stepwise network formation.[71]

Since the molecular distribution of the reacting system is known exactly in terms of the number of monomer units in each of the five reacted states $A_1-A_5$ in each macromolecule, both kinetic and structural information is available after each reaction step. Such information includes the exact values of conversion, kinetic chain length, number of intermolecular and intramolecular (cyclization) reactions, number of initiator decomposition, propagation, and termination reactions, number of radicals, number of cross-links, number of macromolecules, number of pendant double bonds, and number of completely reacted double bonds as a function of reaction time.

## Results and Discussion

Simulations were performed to obtain kinetic and structural information on the process of network formation during a bulk diffusion-controlled tetrafunctional photopolymerization. The initial distribution contained 10 million monomer molecules and 100 000 initiator molecules which was chosen to represent a reaction mixture containing monomer and 1% initiator. The parameters required in the kinetic model were the same as used earlier[67] and are given in Table 2. Simulations were performed using the same set of seed values to initialize the random number generator at each chosen light intensity. The cpu times required were approximately 8 h for the simulation at 0.1 mW/cm$^2$ on a Sun Sparcstation 2 and 14 h for the simulations at 1 mW/cm$^2$ on a HP 9000/755 workstation.

**Table 2. Values of the Parameters Required in the Kinetic Model Used in the Simulation**

| | |
|---|---|
| $N_0 = 10$ million | $A_0 = 100\,000$ |
| $\epsilon = 100$ L/(mol cm) | $T = 30$ °C |
| $v_{fm} = 0.115$ | $v_{fp} = 0.025$ |
| $v_m = 0.9$ cm$^3$/g | $v_p(T,0) = 0.8$ cm$^3$/g |
| $R = 4.5$ Å | |
| $D_0$ (monomer) = 44 cm$^2$/s | $E = 9253$ cal/mol |
| $R = 1.987$ cal/(mol K) | $D_0$ (radical) = 440 cm$^2$/s |
| $\hat{V}_1^* = 0.5$ cm$^3$/g | $\hat{V}_2^* = 0.9$ cm$^3$/g |
| $\xi = 0.9$ | $\delta = 0.94$ |
| $\gamma = 0.9$ | |
| $\phi' = 1$ | $k_{i,1} = 1.32 \times 10^3$ cm/s |
| $k_{d,r,1} = 10^{11}$ s$^{-1}$ | $a = 10$ Å |
| $k_{p,1} = 10^8$ L/(mol s) | |

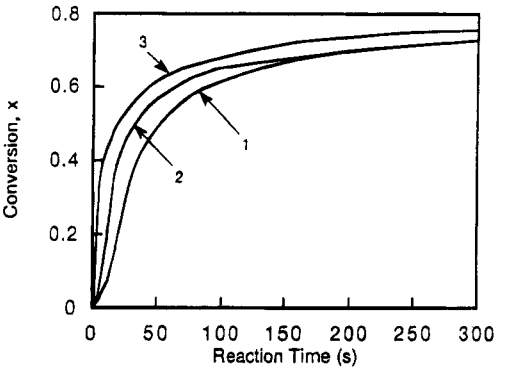


**Figure 2.** Simulation results of the acryl group conversion, $x$, as a function of reaction time at three UV light intensities: 0.02 (curve 1), 0.1 (curve 2), and 1 mW/cm$^2$ (curve 3).

In order to determine the influence of the seed values on the results, three simulations were carried out at the same light intensity of 0.1 mW/cm$^2$ but with different seed values used to initialize the random number generators. Though there was a slight dependence of the conversion–time profiles on the seed values, the trends were the same. Therefore, in the simulations carried out at other light intensities only one set of seed values was used. In future simulations when the quantitative analysis of results is necessary, the results of several runs using different seed values should be averaged.

Figure 2 shows the fractional conversion of the acryl groups as a function of reaction time when simulations were carried out at three light intensities: 0.02, 0.1, and 1 mW/cm$^2$. Since each monomer unit in the $A_1$ or $A_3$ state possesses one reacted acryl group, and each monomer unit in the $A_2$, $A_4$, or $A_5$ state possesses two reacted acryl groups, the conversion can be calculated from a knowledge of the number of monomer units in each of the reacted states in every macromolecule present in the reacting system.

At each light intensity, it was seen that initially the conversion increased rapidly and then began to approach a constant value. In each case, the limiting conversion was less than 100%. This is because, as the reaction proceeded and polymer was formed, the mobility of the reaction species decreased, therefore causing a decrease in the total reaction rate. This decrease in turn caused an increase in the waiting time beyond the time scale of the simulation.

It was also observed that as the light intensity was increased, the limiting conversion was approached more

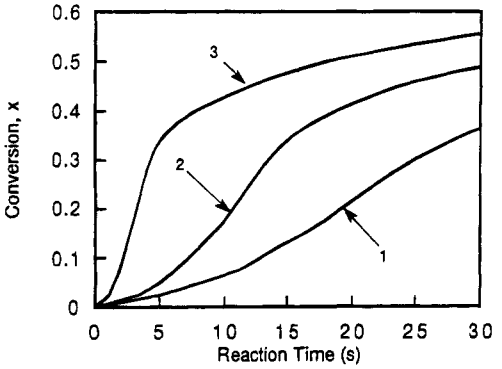


**Figure 3.** Simulation results of the acryl group conversion, $x$, as a function of initial reaction time at three UV light intensities: 0.02 (curve 1), 0.1 (curve 2), and 1 mW/cm$^2$ (curve 3). The S-shaped profiles obtained indicate autoacceleration.

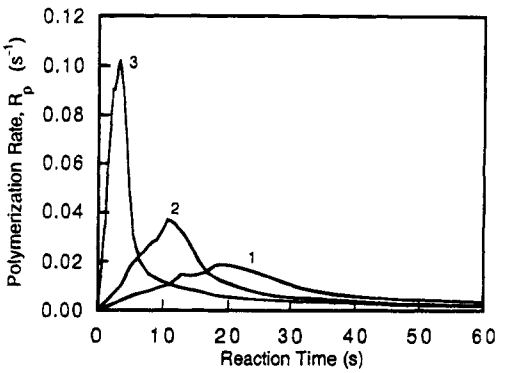


**Figure 4.** Simulation results for the polymerization rate, $R_p$, plotted as a function of reaction time at three UV light intensities: 0.02 (curve 1), 0.1 (curve 2), and 1 mW/cm$^2$ (curve 3). The reaction rate is plotted as a fraction of the double bonds consumed per second. An increase in light intensity increased the initial and peak reaction rate.

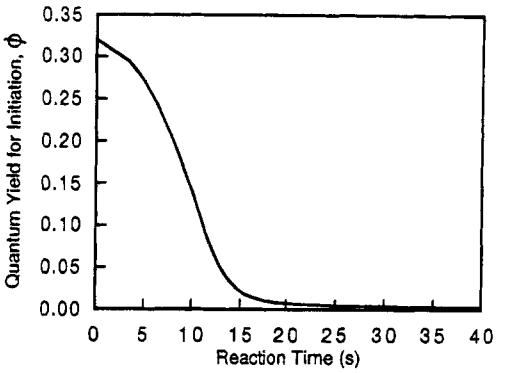


**Figure 5.** Simulation results for the quantum yield of initiation, $\phi$, as a function of time for a polymerization initiated with a UV light intensity of 0.1 mW/cm$^2$. Since $\phi = f\phi'$, the decrease in the quantum yield also shows the decrease in the initiator efficiency, $f$.

rapidly. However, the limiting conversion which was attained beyond the time scale of Figure 2 did not significantly increase with an increase in the incident light intensity as has been observed in experiments.[1,56] This increase is caused by the presence of a temporary excess free volume in the reaction mass which results from a lag between the reaction rate and the volume shrinkage rate. This effect was not incorporated in the present work due to difficulties in the calculation of the contribution of the relaxation of a single macromolecule toward the volume relaxation process, and therefore the limiting conversion did not increase with light intensity in the simulations.

In cross-linking polymerizations, autoacceleration is often observed.[72,73] Autoacceleration defines the phenomena in which the reaction rate increases under isothermal conditions though the monomer concentration is continuously decreasing. This phenomena was observed in the results of the reaction simulations (see Figure 3), as is seen in the S-shaped profiles obtained when the conversion was plotted as a function of the initial reaction time at the three light intensities used in the simulations: 0.02, 0.1, and 1 mW/cm$^2$. An S-shaped profile indicated an increase in the reaction rate during the reaction. As the light intensity was increased, the onset of autoacceleration occurred at an earlier time. Also, the conversion level at which autoacceleration was observed decreased with an increase in light intensity. These effects were the result of an increase in the initiation rate.

Figure 4 shows the theoretical values for the reaction rates as a function of time at three light intensities: 0.02, 0.1, and 1 mW/cm$^2$. The reaction rate was calculated by a finite-difference differentiation of the conversion–time profiles at each light intensity. The profiles indicate all the experimentally observed trends recorded during the bulk photopolymerization of diethylene glycol diacrylate.[56] The simulation results showed that the initial reaction rate and the peak reaction rate increased with an increase in light intensity. Also, the time at which the peak reaction rate was observed decreased from 19 s when the UV light intensity was 0.02 mW/cm$^2$ to 11 s at 0.1 mW/cm$^2$ and 3 s at 1 mW/cm$^2$.

The results of the simulations also showed that the conversion level when the peak reaction rate was reached was approximately 20% in each case and independent of the variation in light intensity. This behavior has been reported in the polymerization of diethylene glycol diacrylate[56] and tetraethylene glycol diacrylate.[9] Such behavior may be due to the fact that diethylene glycol diacrylate is a flexible monomer and therefore the equilibrium volume was maintained before the maximum rate is reached. Since only the equilibrium volume was calculated in the model used for the simulation, the results were in agreement with experimental observations.

The kinetic model incorporated a conversion-dependent initiator efficiency, $f$. A plot of the quantum yield of initiation, $\phi$, as a function of polymerization time when a light intensity of 0.1 mW/cm$^2$ was used for initiation is shown in Figure 5. Since $\phi = f\phi'$ where $\phi'$ is a constant, this plot also shows the decrease in the initiator efficiency, $f$. The decrease in the term $f$ with time and therefore with conversion was a result of the diffusional limitations on the primary radicals formed on initiator decomposition. The efficiency decreased throughout the polymerization process and approached a value $^1/_{10}$th of its initial value in 15 s. Such a sharp decrease in $f$ has been reported by Shen *et al.*[59] who carried out electron spin resonance spectroscopic studies of azobis(isobutyronitrile)-initiated methyl methacrylate polymerizations. These results indicated that in the late stages of the reaction, the rate of chain initiation was negligible since most of the primary radicals formed underwent radical recombination reactions and formed inactive initiator molecules.

A rapid increase in the number of radicals in the reacting system was observed at the onset of the polymerization, as shown in Figure 6 where the number of radicals is plotted as a function of time for polymer-

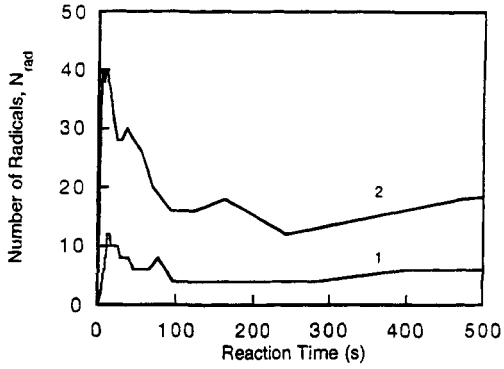


**Figure 6.** Simulation results for the number of radicals, $N_{rad}$, plotted as a function of polymerization time when the reaction was initiated using a UV light intensity of 0.1 (curve 1) and 1 mW/cm$^2$ (curve 2). The leveling off in the number of radicals at late states of the reaction indicates the presence of trapped radicals.

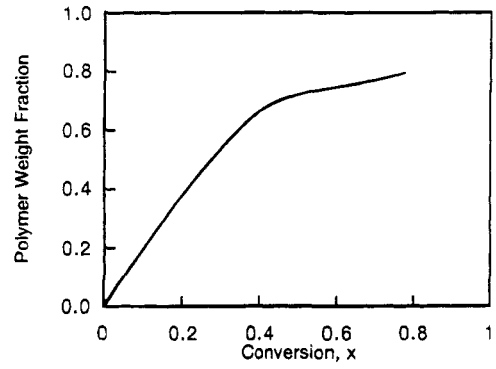


**Figure 7.** Simulation results for the weight fraction of polymer, $\omega_p$, as a function of the (meth)acryl group conversion when a UV light intensity of 0.1 mW/cm$^2$ was used for photoinitiation.

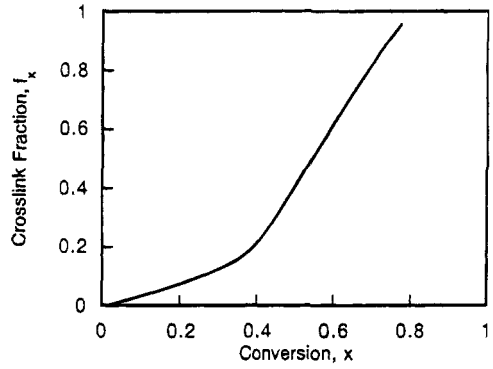


**Figure 8.** Simulation results for the number of cross-links per monomer unit in the polymer molecules, $f_x$, as a function of (meth)acryl group conversion when a UV light intensity of 0.1 mW/cm$^2$ was used for photoinitiation.

izations initiated at UV light intensities of 0.1 and 1 mW/cm$^2$. The profiles obtained were similar to those reported earlier using a mean field model.[67] Initially, the rate of chain initiation, was greater than the rate of termination and therefore the fast increase in the number of radicals was due to the formation of radicals that initiate propagating chains. Also, as the light intensity was increased, the rate of chain initiation was increased and therefore a higher radical concentration was attained.

After the rapid increase, the number of radicals decreased. This was because the termination reactions become more frequent due to the availability of terminating radicals and the chain initiation reactions become less frequent due to the decrease in the initiator efficiency. In the late stages of the polymerization process when the reaction rate approached zero, the radical concentration leveled off and then increased slowly when all reactions other than the chain initiation reactions became less frequent. The finite value for the radical concentration might point to the presence of a trapped radical population.

Trapped radicals are those that are surrounded by dead polymer chains so that their mobility is severely limited and are therefore unavailable for further reaction. Experimental evidence indicates that such trapped radicals have long lifetimes[74,75] and lead to structural heterogeneities in the cross-linked networks.[76] The trapped radical concentration increased with an increase in the light intensity which might imply the existence of greater structural heterogeneities in materials photopolymerized using higher initiation rates. These inhomogeneities are usually undesirable in polymers which are used as information storage systems or as biomaterials.

Figure 7 shows the calculated increase in the weight fraction of the polymer as a function of the acryl group conversion when the polymerization was simulated using a light intensity of 0.1 mW/cm$^2$. Initially, there was a rapid increase in the polymer weight fraction and the increase was almost 2 times the change in conversion. This indicated that at the onset of the reaction there was a strong tendency for the acryl groups on the free monomer to react preferentially, as compared to the pendant double bonds so that macromolecular structure was rapidly formed. However, Kloosterboer *et al.*[77] have shown that in the photopolymerization of 1,6-hexanediol diacrylate, at low conversions the pendant double bonds are slightly more reactive than the double bonds on the free monomer. Boots and co-workers[6,42,43] presented a lattice-based percolation model which qualitatively describes such behavior which is a result of the proximity of the active chain ends to pendant double bonds. This space-based effect is difficult to include in an off-space simulation such as the one presented here.

After the fast increase, the polymer weight fraction seemed to level off and did not increase significantly with conversion. This behavior implied that in the later stages of the reaction, pendant double bonds were more reactive than free monomer double bonds. This occurred because at higher conversion levels, the translational diffusivity of the monomer had fallen to a point where the monomer could no longer move easily to a radical site.

The formation of cross-links in the macromolecular structure was followed by calculating the number of cross-links per monomer unit in the polymer molecules, $f_x$, as a function of conversion and is shown in Figure 8 for a reaction initiated using a UV light intensity of 0.1 mW/cm$^2$. A monomer unit that had both double bonds completely reacted was regarded as a cross-link, i.e. a monomer unit in state $A_5$. The figure shows that cross-links were formed from the onset of the reaction. These cross-links can lead to the formation of microgel regions in the reaction matrix that are known to occur in the polymerization of multifunctional monomers.[5,78] After an initial slow increase, the fraction of cross-links in the macromolecules increased rapidly, indicating that in the later stages of the reactions intramolecular reactions became more frequent, leading to the formation of primary and secondary cycles and the reaction of pendant double bonds.

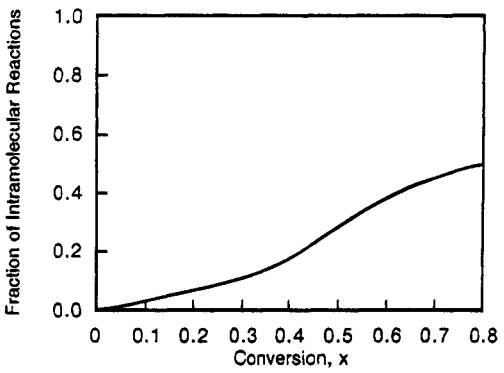


**Figure 9.** Simulation results for the fraction of reactions that were intramolecular, $f_{rxn}$, as a function of (meth)acryl group conversion when a UV light intensity of 0.1 mW/cm$^2$ was used for photoinitiation.

Such a hypothesis can be confirmed by calculating the fraction of reactions that were intramolecular, $f_{rxn}$. This was done by computing the number of reactions that were of types given by reaction numbers 16–27 (see Table 1). A plot of the fraction of intramolecular reactions as a function of conversion when a light intensity of 0.1 mW/cm$^2$ was used for photoinitiation is shown in Figure 9. This figure shows that at low conversions, most of the reactions that occur were intermolecular and involved the reaction of free monomer molecules with active chain ends. However, as the reaction proceeded, intramolecular reactions became more frequent as the translational diffusivity of the monomer molecules decreased. This led to the formation of cross-links and the increased consumption of pendant double bonds. The dependence of the fraction of intramolecular reactions on the systems' size is still to be investigated.

## Conclusions

A Monte Carlo off-space technique was developed for the simulation of the bulk photopolymerization of a tetrafunctional monomer. The kinetic model that was used in the simulation incorporated a diffusion-dependent initiator efficiency and propagation and termination rate constants. Simulation results were able to provide both kinetic and structural information about the network formation process. This information was in agreement with experimentally observed reaction trends. Autoacceleration was observed, the magnitude of which increased as the light intensity was increased. An increase in the initial and peak reaction rate with an increase in light intensity was also observed. The initiator efficiency decreased as the reaction progressed due to diffusional limitations on the radicals formed on initiator decomposition. A trapped radical population was observed which increased with an increase in light intensity which may point to the existence of greater structural heterogeneities in materials photopolymerized at higher light intensities.

However, two features observed in cross-linking photopolymerizations were not predicted. One of them is the increase in limiting conversion with an increase in the photoinitiation rate; the other is the preferential reaction of pendant double bonds as compared to the double bonds of the free monomer at low conversions. Incorporation of the effect of volume relaxations and the space-based effect of the nearness of the active chain ends to pendant double bonds will allow these features to be predicted. Future efforts will concentrate in this direction.

**Acknowledgment.** Financial support from the National Science Foundation (Grant No. CTS-93-11563) and a Global Initiative Grant from Purdue University is gratefully acknowledged. D.K. is thankful for a stay at the Institute of Macromolecular Chemistry in Prague.

## References and Notes

(1) Kloosterboer, J. G. *Adv. Polym. Sci.* **1988**, *84*, 1.
(2) Turner, D. T.; Hague, Z. U.; Kalachandra, S.; Wilson, T. W. *Polym. Mater. Sci. Eng. Proc.* **1987**, *56*, 769.
(3) Peppas, N. A.; Langer, R. *Science* **1994**, *263*, 1715.
(4) Dušek, K. In *Developments in Polymerization*; Haward, R. N., Ed.; Applied Sciences: London, 1982; p 143.
(5) Dušek, K.; Spevaček, J. *Polymer* **1980**, *21*, 750.
(6) Boots, H. M. J.; Kloosterboer, J. G.; van de Hei, G. M. M.; Pandey, R. B. *Br. Polym. J.* **1985**, *17*, 219.
(7) Marten, F. L.; Hamielec, A. E. In *Polymerization Reactors and Processes*; Henderson, J. N., Bouton, T. C., Eds.; American Chemical Society: Washington, DC, 1979; p 43.
(8) Chern, C. S.; Poehlein, G. W. *Polym. Plast. Technol. Eng.* **1990**, *29*, 577.
(9) Bowman, C. N.; Peppas, N. A. *Macromolecules* **1991**, *24*, 1914.
(10) Soh, S. K.; Sundberg, D. C. *J. Polym. Sci., Polym. Chem. Ed.* **1982**, *20*, 1299.
(11) Soh, S. K.; Sundberg, D. C. *J. Polym. Sci., Polym. Chem. Ed.* **1982**, *20*, 1315.
(12) Soh, S. K.; Sundberg, D. C. *J. Polym. Sci., Polym. Chem. Ed.* **1982**, *20*, 1331.
(13) Soh, S. K.; Sundberg, D. C. *J. Polym. Sci., Polym. Chem. Ed.* **1982**, *20*, 1345.
(14) Batch, G.; Macosko, C. *J. Appl. Polym. Sci.* **1992**, *44*, 1711.
(15) Williams, R. J. J.; Vallo, C. I. *Macromolecules* **1988**, *21*, 2571.
(16) Dotson, N. A. *Macromolecules* **1992**, *25*, 308.
(17) Tobita, H.; Hamielec, A. E. In *Computer Applications in Applied Polymer Science II*; Provder, T., Ed.; American Chemical Society: Washington, DC, 1989; p 242.
(18) Tobita, H.; Hamielec, A. E. *Macromolecules* **1989**, *22*, 3098.
(19) Tobita, H.; Hamielec, A. E. *Polymer* **1992**, *33*, 3647.
(20) Tobita, H. *Makromol. Chem. Theory Simul.* **1993**, *2*, 761.
(21) Tobita, H. *Macromolecules* **1993**, *26*, 5427.
(22) Flory, P. J. *Principles of Polymer Chemistry*; Cornell University Press: Ithaca, NY, 1953.
(23) Stockmayer, W. H. *J. Chem. Phys.* **1943**, *11*, 45.
(24) Mikos, J.; Dušek, K. *Macromolecules* **1982**, *15*, 93.
(25) Šomvársky, J.; Dušek, K. *Polym. Bull.* **1994**, *33*, 369.
(26) Dušek, K. *Makromol Chem., Suppl.* **1979**, *2*, 35.
(27) Dušek, K.; Ilávsky, M. *J. Polym. Sci., Polym. Symp.* **1975**, *53*, 57.
(28) Dušek, K.; Ilávsky, M. *J. Polym. Sci., Polym. Symp.* **1975**, *53*, 75.
(29) Sarmoria, C.; Miller, D. R. *Macromolecules* **1990**, *23*, 580.
(30) Dotson, N. A.; Macosko, C. W.; Tirrell, M. In *Synthesis Characterization and Theory of Polymeric Networks and Gels*; Aharoni, W. M., Ed.; Plenum Press: New York, 1992; p 319.
(31) Tobita, H. *Macromolecules* **1992**, *25*, 2671.
(32) Dotson, N. A.; Galvan, R.; Macosko, C. W. *Macromolecules* **1988**, *21*, 2560.
(33) Tobita, H.; Hamielec, A. E. *Macromol. Symp.* **1988**, *20/21*, 501.
(34) Scranton, A. B.; Peppas, N. A. *J. Polym. Sci., Polym. Chem. Ed.* **1990**, *28*, 39.
(35) Dušek, K.; Šomvársky, J. In *Synthesis, Characterization, and Theory of Polymeric Networks and Gels*; Aharoni, S. M., Ed.; Plenum Press: New York, 1992; p 283.
(36) Manneville, P.; de Seze, L. In *Numerical Methods in the Study of Critical Phenomena*, Dora, J. D., Demongeot, J., Lacolle, B., Eds.; Springer Verlag: Berlin, 1981; p 116.
(37) Romiszowski, R.; Kolinsy, A. *Polymer* **1982**, *23*, 1226.
(38) Leung, Y. K.; Eichinger, B. E. *J. Chem. Phys.* **1984**, *80*, 3877.
(39) Leung, Y. K.; Eichinger, B. E. *J. Chem. Phys.* **1984**, *80*, 3885.
(40) Rohr, D. F.; Klein, M. T. *Ind. Eng. Chem. Res.* **1990**, *29*, 1210.
(41) Gupta, A. M.; Hendrickson, R. C.; Macosko, C. W. *J. Chem. Phys.* **1991**, *95*, 2097.
(42) Boots, H. M. J.; Pandey, R. B. *Polym. Bull.* **1984**, *11*, 415.
(43) Boots, H. M. J. In *Integration of Fundamental Polymer Science and Technology*; Kleintjens, L. A., Lemstra, P. J., Eds.; Elsevier: London, 1985; p 204.
(44) Boots, H. M. J. In *Biological and Synthetic Polymer Networks*; Kramer, O., Ed.; Elsevier: London, 1988; p 267.
(45) Simon, G. P.; Allen, P. E. M.; Bennett, D. J.; Williams, D. R. G.; Williams, E. H. *Macromolecules* **1989**, *22*, 3555.

(46) Bansil, R.; Herrmann, H. J.; Stauffer, D. *Macromolecules* **1984**, *17*, 998.
(47) Bowman, C. N.; Peppas, N. A. *Chem. Eng. Sci.* **1992**, *46*, 1411.
(48) Romantsova, I. I. *Int. J. Polym. Mater.* **1993**, *19*, 51.
(49) Koshiro, Y.; Ma, G. H.; Fukutomi, T. *Polym. Gels Networks* **1994**, *2*, 29.
(50) Chiu, Y. Y.; Lee, L. J. *J. Polym. Sci., Polym. Chem. Ed.* **1995**, *33*, 269.
(51) Gillespie, D. T. *J. Comput. Phys.* **1976**, *22*, 403.
(52) Gillespie, D. T. *J. Phys. Chem.* **1977**, *81*, 2340.
(53) Gardiner, C. W. *Handbook, of Stochastic Methods*; Springer-Verlag: Berlin, Germany, 1985.
(54) Lu, J.; Zhang, H.; Yulian, Y. *Makromol. Chem. Theory Simul.* **1993**, *2*, 747.
(55) Cheng, K. C.; Chiu, W. Y. *Macromolecules* **1994**, *27*, 3406.
(56) Kurdikar, D. L.; Peppas, N. A. *Polymer* **1994**, *35*, 1004.
(57) Sandner, M. R.; Osborn, C. L. *Tetrahedron Lett.* **1974**, *5*, 415.
(58) Groenenboom, C. J.; Hageman, H. J.; Overeem, T.; Weber, A. J. M. *Makromol. Chem.* **1982**, *183*, 281.
(59) (a) Shen, J. C.; Tian, Y.; Wang, G. B.; Yang, M. L. *Sci. China (B)* **1990**, *33*, 1046. (b) Shen, J. C.; Tian, Y.; Wang, G.; Yang, M. *Makromol. Chem.* **1991**, *192*, 2669.
(60) Russell, G. T.; Napper, D. H.; Gilbert, R. G. *Macromolecules* **1988**, *21*, 2141.
(61) Kurdikar, D. L.; Peppas, N. A. *Macromolecules* **1994**, *27*, 733.
(62) Vrentas, J. S.; Vrentas, C. M. *J. Appl. Polym. Sci.* **1991**, *42*, 1931.
(63) Rice, S. *Diffusion-Limited Reactions*; Elsevier: New York, 1985.
(64) Vrentas, J. S.; Duda, J. L. *J. Polym. Sci., Polym. Phys. Ed.* **1977**, *15*, 403.
(65) Vrentas, J. S.; Duda, J. L. *J. Polym. Sci., Polym. Phys. Ed.* **1977**, *15*, 417.
(66) de Gennes, P. G. *Scaling Concepts in Polymer Physics*; Cornell University Press: Ithaca, NY, 1979; p 227.
(67) Kurdikar, D. L.; Peppas, N. A. *Macromolecules* **1994**, *27*, 4084.
(68) Mahabadi, H. K.; O'Driscoll, K. F. *Macromolecules* **1977**, *10*, 55.
(69) Dušek, K.; MacKnight, W. J. In *Crosslinked Polymers Chemistry, Properties and Applications*; Dickie, R. A., Labana, S. S., Bauer, R. S., Eds.; American Chemical Society: Washington, DC, 1988; p 2.
(70) Tsou, A. H.; Peppas, N. A. *J. Polym. Sci., Polym. Phys. Ed.* **1988**, *26*, 2043.
(71) Šomvársky, J.; Dušek, K. *Polym. Bull.* **1994**, *33*, 377.
(72) Li, W. H.; Hamielec, A. E.; Crowe, C. M. *Polymer* **1989**, *30*, 1513.
(73) Scranton, A. B.; Bowman, C. N.; Klier, J.; Peppas, N. A. *Polymer* **1992**, *33*, 1683.
(74) Kloosterboer, J. G.; Lijten, G. F. C. M. In *Biological and Synthetic Polymer Networks*; Kramer, O., Ed.; Elsevier: London, 1988; p 345.
(75) Bellobono, I. R.; Oliva, C.; Morelli, R.; Selli, E.; Ponti, A. *J. Chem. Soc., Faraday Trans.* **1990**, *86*, 3273.
(76) Zhu, S.; Tian, Y.; Hamielec, A. E.; Easton, D. R. *Polymer* **1990**, *31*, 154.
(77) Kloosterboer, J. G.; Lijten, G. F. C. M.; Boots, H. M. J. *Makromol. Chem. Macromol. Symp.* **1989**, *24*, 223.
(78) Dušek, K.; Galina, H.; Mikes, J. *Polym. Bull.* **1980**, *3*, 19.

MA9463425